AIAA JOURNAL
Vol. 43, No. 3, March 2005

Use of Arc-Length Method for Capturing Mode Jumping in Postbuckling Aerostructures

Marco Cerini* and Brian G. Falzon†
Imperial College London, London, England SW7 2AZ, United Kingdom

The arc-length method has become a widely established solution technique for studying nonlinear structural behavior. By augmenting the set of nonlinear equilibrium equations with a constraint equation, which is a function of both the displacements and load increment, it is capable of traversing limit points. Numerous investigations have shown that highly nonlinear behavior such as sharp "snap-backs" can still lead to numerical difficulties. Two practical examples are presented to assess the effectiveness of this solution technique in capturing secondary instabilities in postbuckling structures, which present themselves as abrupt mode jumps. Although the first example poses no special difficulties, in the second case the nonlinear procedure fails to converge. An improvement to the method's formulation is suggested, which accounts for the residual forces that are usually neglected, when proceeding to the next increment once convergence is reached on the current increment. The choice of a correct load increment at the first iteration, within a predictor-corrector scheme, is central to the method's effectiveness. Current strategies for a choice of this load increment are discussed and are shown to be no longer consistent with the modified formulation; therefore, a new approach is proposed.

Introduction

THE dominant form of airframe construction is characterized by a thin skin, which primarily acts as a membrane and forms the aerodynamic surface, stabilized under compression by the use of stiffeners or stringers. Experimental investigations on metallic and carbon-fiber composite stiffened panels, loaded in uniaxial compression, have shown the ability of these panels to support load beyond the initial buckling of the skin.[1–6] Hence, it is generally accepted that stiffened aerostructures can be designed to support load beyond buckling. This design philosophy has been adopted for metallic airframe construction where certain structural components are allowed to buckle between the design limit and ultimate loads. Such postbuckling designs are at least 10% lighter than their nonbuckling counterparts. Indeed, internal structural components, which do not have a significant bearing on the aerodynamic surface properties, can be designed to buckle below the design limit load. A postbuckling design philosophy has yet to be widely adopted in the design of composite airframes. This is primarily because of the relatively low through-thickness strength of composite laminates, which makes stiffened structures prone to premature skin-stiffener debonding in cocured or secondary-bonded structures.

A further complication also arises. Various experimental studies have shown that when these panels are loaded beyond their initial buckling loads they can undergo a secondary instability resulting in an abrupt mode-shape change. At high loading, these sudden changes can release enough energy to cause damage on first occurrence.[7] Bushnell et al.[8] have shown that even though a mode jump might involve only a small change in potential energy, it generates large-amplitude oscillating stresses with significant stress reversal. This can give rise to fatigue problems if it occurs often or can lead to delamination.[9] It thus becomes clear that the design of postbuckling structures must include the analytical capability of capturing these secondary instabilities.

Received 28 January 2004; revision received 3 October 2004; accepted for publication 11 October 2004.

*Ph.D. Student, Department of Aeronautics, South Kensington Campus; marco.cerini@imperial.ac.uk. Student Member AIAA.

†Lecturer, Department of Aeronautics, South Kensington Campus; b.falzon@imperial.ac.uk. Member AIAA.

The arc-length method has been widely used in recent years to model highly nonlinear behavior. This paper provides a systematic treatment of the use of the arc-length method to capture mode jumping. The method is based on augmenting the system of nonlinear equilibrium equations with an additional constraint equation that limits the increment to an arc length which is a function of both the incremental displacements and incremental load. Two examples of arc-length analyses of postbuckling shell structures are presented in order to investigate the capabilities and robustness of the method in detecting mode jumps. Both the general case of a simply supported rectangular plate made of isotropic material and the more specialized case of a composite stiffened panel are considered. These two examples also highlight some drawbacks of the nonlinear solution technique.

In standard formulations,[10–13] the predictor and subsequent correctors are determined with different sets of equations, mainly because the predictor is considered as the tangential solution from an equilibrium state, whereas the starting point in correctors is a nonequilibrium state. It is shown, however, that this established practice of ignoring the residual in proceeding to the next increment once the current increment has achieved convergence within a set tolerance can prevent convergence near sharp limit points. The reason for this failure is explained in detail and demonstrated by means of a numerical example.

Central to the arc-length method's effectiveness is the ability to choose an incremental load parameter that does not double back on itself where the solution converges to previously computed points on the equilibrium path. Current techniques available for a suitable choice of load increment are discussed. It is shown that they are not consistent with a predictor accounting for the residual force, and therefore a new approach is proposed.

Arc-Length Method

In structural analysis where the applied load varies very slowly and entails slow changes of configuration, it is possible to neglect viscous and inertia forces. This situation is usually referred to as a quasi-static condition. Under quasi-static conditions the nonlinear response of a discretized structural system can therefore be described by the following equilibrium equation:

$$\boldsymbol{g}(\boldsymbol{u}, \boldsymbol{r}) := \boldsymbol{f}(\boldsymbol{u}) - \boldsymbol{r} = 0 \tag{1}$$

where $\boldsymbol{g}$ represents the residual force vector, expressed as the difference between the internal force vector $\boldsymbol{f}$, function of the displacement variables $\boldsymbol{u}$, and the external force vector $\boldsymbol{r}$.

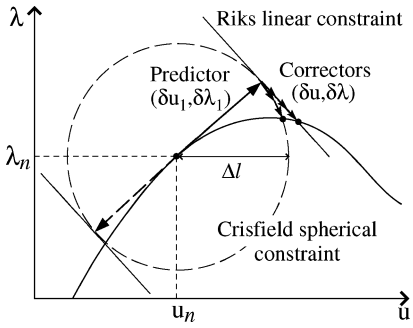

Fig. 1 Riks and Crisfield arc-length methods.

The continuous sequence of equilibrium states corresponding to a continuous variation of load traces out an equilibrium path in the displacement-load space. If the undeformed state belongs to an equilibrium path, this is also called the fundamental path. When the intensity of the load is controlled by a single parameter λ that multiplies a fixed load vector $\bar{\boldsymbol{r}}$, such that $\boldsymbol{r} = \lambda\bar{\boldsymbol{r}}$, and the configuration space has dimension N, an equilibrium path can be regarded as a line in a space of dimension $N+1$, and the residual force as $\boldsymbol{g} = \boldsymbol{g}(\boldsymbol{u}, \lambda)$.

Arc-length methods, first introduced by Wempner[10] and Riks,[11,14] are able to trace an equilibrium path by means of a predictor-corrector (or incremental-iterative) procedure. Starting from a known equilibrium configuration $(\boldsymbol{u}_n, \lambda_n)$ obtained at increment n, as shown in Fig. 1, an estimate for a subsequent equilibrium point on the curve is determined as the tangential solution, which lies at a prescribed distance Δl from the current position. By means of further Newton iterations, this initial estimate can be improved in order to match a desired tolerance. Arc-length methods, therefore, typically combine the equilibrium equation (1) with a path-constraint equation that fixes the step size of each increment.

Wempner and Riks techniques are very similar because both make use of a linear constraint. If $(\delta\boldsymbol{u}_1^*, \delta\lambda_1^*)$ is the tangential direction at the beginning of an increment and it is normalized as follows:

$$\delta\boldsymbol{u}_1^* \cdot \delta\boldsymbol{u}_1^* + \left(\delta\lambda_1^*\right)^2 = 1 \tag{2}$$

The path constraint suggested by Riks is a hyperplane orthogonal to $(\delta\boldsymbol{u}_1^*, \delta\lambda_1^*)$. At the predictor stage, which is the first iteration within an increment, combining the linearization of the equilibrium path about the current equilibrium state with the constraint suggested by Riks, yields the following system:

$$\frac{\partial \boldsymbol{g}}{\partial \boldsymbol{u}}\delta\boldsymbol{u}_1 + \frac{\partial \boldsymbol{g}}{\partial \lambda}\delta\lambda_1 = \boldsymbol{0} \tag{3}$$

$$\delta\boldsymbol{u}_1^* \cdot \delta\boldsymbol{u}_1 + \delta\lambda_1^*\delta\lambda_1 = \Delta l \tag{4}$$

where $\delta\boldsymbol{u}_1$ and $\delta\lambda_1$ are predictor changes in the current increment and Δl is the prescribed arc-length increment.

Unlike a predictor, where a linearization of the equilibrium path is considered, corrector iterations aim at minimizing the residual force. Therefore the residual force about the current nonequilibrium state is linearized and equated to zero:

$$\begin{aligned}\boldsymbol{g}(\boldsymbol{u}+\delta\boldsymbol{u}, \lambda+\delta\lambda) &\approx \boldsymbol{g}(\boldsymbol{u}, \lambda) + \frac{\partial \boldsymbol{g}}{\partial \boldsymbol{u}}\delta\boldsymbol{u} + \frac{\partial \boldsymbol{g}}{\partial \lambda}\delta\lambda \\ &= \boldsymbol{g} + \boldsymbol{K}_t\delta\boldsymbol{u} - \bar{\boldsymbol{r}}\delta\lambda = \boldsymbol{0}\end{aligned} \tag{5}$$

Here $\boldsymbol{K}_t$ is the tangent stiffness matrix of the system, and use has been made of the equivalence:

$$\boldsymbol{K}_t := \left[\frac{\partial \boldsymbol{f}}{\partial \boldsymbol{u}}\right] = \left[\frac{\partial \boldsymbol{g}}{\partial \boldsymbol{u}}\right] \tag{6}$$

The following system combines Eq. (5) with Riks constraint:

$$\frac{\partial \boldsymbol{g}}{\partial \boldsymbol{u}}\delta\boldsymbol{u} + \frac{\partial \boldsymbol{g}}{\partial \lambda}\delta\lambda = -\boldsymbol{g} \tag{7}$$

$$\delta\boldsymbol{u}_1 \cdot \delta\boldsymbol{u} + \delta\lambda_1\delta\lambda = 0 \tag{8}$$

and its solution yields the corrector changes $\delta\boldsymbol{u}$ and $\delta\lambda$.

Because the predictor is tangential and therefore $(\delta\boldsymbol{u}_1, \delta\lambda_1) = \Delta l(\delta\boldsymbol{u}_1^*, \delta\lambda_1^*)$, Eq. (4) is in fact a quadratic equation and is very similar to Crisfield's predictor, which is illustrated next. Riks also describes a method to establish whether a critical state is a limit or a bifurcation point and shows how to determine the equilibrium path past a bifurcation point that exhibits one single zero eigenvalue.[11]

Crisfield's method[12] differs from the preceding one in that a quadratic arc-length constraint is employed also for corrector iterations. The following equation is adopted for the predictor:

$$a(\delta\boldsymbol{u}_1, \delta\lambda_1) := \left(\delta\boldsymbol{u}_1 \cdot \delta\boldsymbol{u}_1 + \psi^2\delta\lambda_1^2\bar{\boldsymbol{r}} \cdot \bar{\boldsymbol{r}}\right) - \Delta l^2 = 0 \tag{9}$$

and similarly for correctors:

$$a(\Delta\boldsymbol{u} + \delta\boldsymbol{u}, \Delta\lambda + \delta\lambda) = 0 \tag{10}$$

where $\Delta\boldsymbol{u}$ and $\Delta\lambda$ are the cumulative changes in the current increment accounting for the predictor and all previous correctors. Equations (9) and (10) both trace a hypersphere of radius Δl and centered at $(\boldsymbol{u}_n, \lambda_n)$. When the contribution of the external force $\boldsymbol{r}$ is neglected by setting the load-scaling parameter ψ to zero, the method is referred to as cylindrical.

If the quadratic equation (10) is linearized as follows:

$$\frac{\partial a}{\partial \boldsymbol{u}}\delta\boldsymbol{u} + \frac{\partial a}{\partial \lambda}\delta\lambda = -a \tag{11}$$

and combined with Eq. (7), the following linear system is obtained:

$$\begin{Bmatrix}\delta\boldsymbol{u} \\ \delta\lambda\end{Bmatrix} = -\begin{bmatrix}\boldsymbol{K}_t & -\bar{\boldsymbol{r}} \\ 2\Delta\boldsymbol{u}^T & 2\Delta\lambda\psi^2\bar{\boldsymbol{r}} \cdot \bar{\boldsymbol{r}}\end{bmatrix}^{-1}\begin{Bmatrix}\boldsymbol{g} \\ a\end{Bmatrix} \tag{12}$$

This system results in an augmented bordered stiffness matrix, which is neither symmetric nor banded, hence not directly amenable to usual finite element solvers. Using an alternative approach suggested by Batoz and Dhatt,[15] from Eq. (5) $\delta\boldsymbol{u}$ is expressed as a function of $\delta\lambda$ and split into two parts:

$$\delta\boldsymbol{u} = \delta\tilde{\boldsymbol{u}} + \delta\lambda\hat{\boldsymbol{u}} \tag{13}$$

where $\delta\tilde{\boldsymbol{u}} = -\boldsymbol{K}_t^{-1}\boldsymbol{g}$ is the iterative change arising from a load-control Newton–Raphson technique and $\hat{\boldsymbol{u}} = \boldsymbol{K}_t^{-1}\bar{\boldsymbol{r}}$ is the displacement from the fixed loading $\bar{\boldsymbol{r}}$. The two solutions can then be found simply by solving the quadratic scalar equation in $\delta\lambda$ obtained after substitution of relation (13) into constraint (10). Following this approach, only the standard banded and symmetric stiffness matrix $\boldsymbol{K}_t$ needs to be inverted.

Whenever a quadratic constraint is adopted, a criterion to select either solution is required. Various criteria have been suggested in the literature, which differ for predictor and correctors. For corrector iterations, the authors have found that the criterion suggested by Hellweg and Crisfield[16] proved very reliable even in the presence of sharp snap-back behavior. This method involves selecting the solution that yields the smaller residual norm:

$$\delta\lambda = \delta\lambda_i \Leftrightarrow \|\boldsymbol{g}(\boldsymbol{u}_i, \lambda_i)\| < \|\boldsymbol{g}(\boldsymbol{u}_j, \lambda_j)\| \tag{14}$$

where subscripts i, j refer to either solution of the quadratic constraint and $\boldsymbol{u}_i = \boldsymbol{u} + \Delta\boldsymbol{u} + \delta\boldsymbol{u}_i$ and $\lambda_i = \lambda + \Delta\lambda + \delta\lambda_i$.

Predictor criteria usually assume that the two solutions in $\delta\lambda$ are equal and opposite in sign (Fig. 2). Indeed from Eq. (3) $\delta\boldsymbol{u}_1$ can be expressed as

$$\delta\boldsymbol{u}_1 = \boldsymbol{K}_t^{-1}\bar{\boldsymbol{r}}\,\delta\lambda_1 = \hat{\boldsymbol{u}}\,\delta\lambda_1 \tag{15}$$

In particular, when the cylindrical method is adopted ($\psi = 0$), from predictor constraint (9), the two solutions for the load increment become

$$\delta\lambda_1 = \pm\Delta l \Big/ \sqrt{\hat{\boldsymbol{u}} \cdot \hat{\boldsymbol{u}}} \tag{16}$$

Crisfield[12] suggests setting the sign of $\delta\lambda_1$ in the predictor to follow the sign of the tangent stiffness matrix determinant:

$$\operatorname{sign}(\delta\lambda_1) = \operatorname{sign}(|\boldsymbol{K}_t|) \tag{17}$$

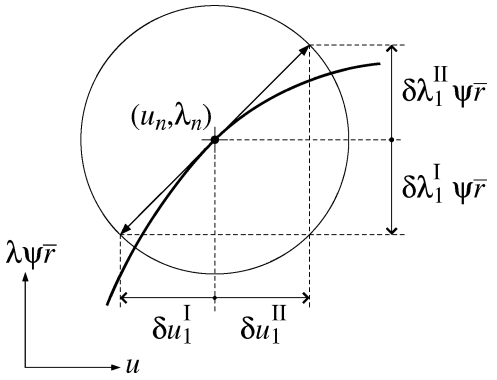

Fig. 2 Predictor solutions.

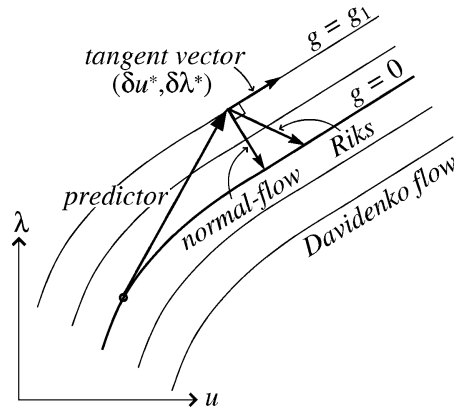

Fig. 3 Normal flow iterate for a one-dimensional system.

De Souza and Feng,[17] alternatively, suggest the use of the sign of the internal product between the incremental displacement resulting from the previous increment $\Delta\boldsymbol{u}_p$ and the current tangential solution $\hat{\boldsymbol{u}}$:

$$\text{sign}(\delta\lambda_1) = \text{sign}(\Delta\boldsymbol{u}_p \cdot \hat{\boldsymbol{u}}) \tag{18}$$

It is further claimed that, using this relationship, the arc-length algorithm is able to overcome bifurcation points. However, whereas limit points can be generally dealt with by an arc-length technique without any additional computations, bifurcation points require knowledge of the eigenvectors of $\boldsymbol{K}_t$ corresponding to the eigenvalues that become zero at that critical state, in order to determine the secondary path that has to be followed thereafter. A technique for dealing with bifurcation points characterized by one single zero eigenvalue is described by Riks.[11] The effect of various criteria on Crisfield's arc-length method has been investigated by the authors,[18] and some examples are provided in the following sections.

Another method worthy of note is known as the normal-flow algorithm: it was introduced in structural mechanics by Fried[13] and was recently investigated by Ragon et al.[19] as a valid alternative to Riks and Crisfield's techniques. Provided a predictor solution is determined with any of the preceding methods, the normal-flow algorithm seeks for the shortest path that leads back onto the equilibrium path, without the need for a specific trajectory constraint. With reference to Fig. 3, the shortest iterative change that tends to displace the system from a state with $\boldsymbol{g} = \boldsymbol{g}_1$ to a state with $\boldsymbol{g} = \boldsymbol{0}$ is also orthogonal to the line $\boldsymbol{g} = \boldsymbol{g}_1$, where the set of lines

$$\boldsymbol{g}(\boldsymbol{u}, \lambda) = \bar{\boldsymbol{g}} \tag{19}$$

with varying $\bar{\boldsymbol{g}}$ is known as the Davidenko flow. If $(\delta\boldsymbol{u}^*, \delta\lambda^*)$ is a vector tangent to the line $\boldsymbol{g} = \boldsymbol{g}_1$ in the current state, the additional equation used in a corrector to constrain Eq. (7) is

$$(\delta\boldsymbol{u}^*, \delta\lambda^*) \cdot (\delta\boldsymbol{u}, \delta\lambda) = 0 \tag{20}$$

Arc-length methods can also be useful for the solution of problems that are not strictly quasi-static, as for example when a structure, albeit subject to a slowly changing load, undergoes a fast dynamic change of configuration. This is the case of snapping structures, as a shallow arch or shell with lateral load. In these cases there exists an unstable equilibrium path that connects the two stable configurations before and after a dynamic event, and that is the reason why an arc-length method can be successfully employed. Once the full equilibrium path has been traced, it is possible to assess whether a branch is stable or unstable and where the dynamic events take place. The behavior of the system during the dynamic phase, however, remains largely unexplored. It has also been suggested[7] that there might be cases in which a dynamic event occurs under quasi-static loading conditions, but a continuous equilibrium path leading to the postcritical configuration does not exist.

Isotropic Plate Loaded in Uniaxial Compression

The arc-length method is employed to study the postbuckling behavior of a rectangular aluminum plate under uniaxial compression, which Stein investigated in his seminal work.[1] An aluminum panel was divided into 11 bays by knife edges, in order to obtain, in the central bay, boundary conditions resembling the ones shown in Fig. 4. The loaded edges were compressed "flat ended" between the platens of a hydraulic testing machine, which resulted in clamped-end conditions. The test was set up such that the nonloaded edges of the central bay were simply supported and remained straight but free to move in plane. The experimental load-shortening curve is given in nondimensional form in Fig. 5. Changes in buckle pattern were detected and are shown as load drops on the curve. The changes occurred abruptly, and the mode shape was observed to go from five to six to seven to eight half-waves.

Stein's experiment on the aluminum plate has been considered by numerous authors as a benchmark to validate analytical or numerical

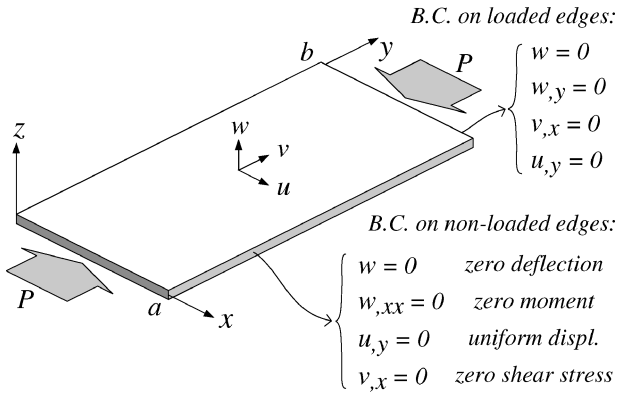

Fig. 4 Mathematical model of Stein's test on an aluminum plate.

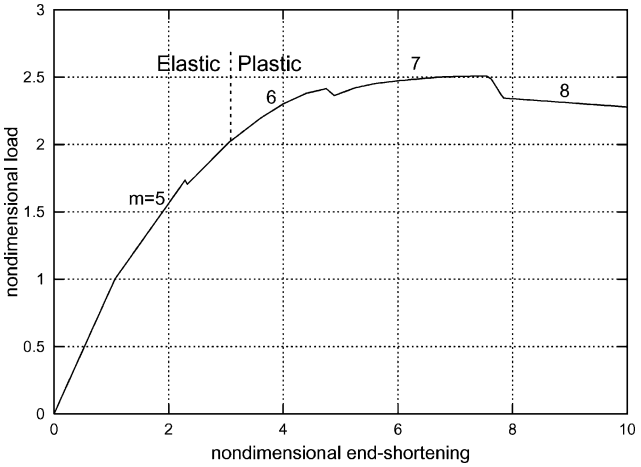

Fig. 5 Experimental load-shortening curve of Stein's test. (The number *m* of half-waves is shown.)

methods.[7,20–23] As will be apparent from the results of the analysis, arc-length control is essential in a quasi-static analysis because of the presence of sharp snap-backs in the equilibrium path.

The analysis was carried out using the commercial finite element package LUSAS,[24] which implements the cylindrical formulation of Crisfield's arc-length method. The tangent stiffness determinant criterion [Eq. (17)] was adopted for predictor iterations and the minimum residual norm criterion [Eq. (14)] for correctors. An initial geometric imperfection was added to the finite element model of the flat plate in order to eliminate bifurcations. After running a linear bucking analysis to determine the eigenvectors $\boldsymbol{a}_i$ of the undeformed configuration, the imperfection $\boldsymbol{w}_0$ was set as a linear combination of the first two eigenmodes:

$$\boldsymbol{w}_0 = \alpha h\,(\boldsymbol{a}_1 + \boldsymbol{a}_2) \tag{21}$$

where h is the plate thickness and α was set to 0.01. Only one eigenmode would be required to remove the first bifurcation point corresponding to primary buckling; however, either a pure symmetric or antisymmetric imperfection would not avoid secondary buckling bifurcations because a new buckle could equally stem from either side of the plate. Therefore the sum of the first, symmetric, and the second, antisymmetric, eigenmode was chosen to obtain an asymmetric initial imperfection.

The plate was modeled with quadrilateral semi-Loof shell elements,[25] which can undergo large displacements and rotations using a total Lagrangian formulation. The isotropic material was considered linear elastic. The employed finite element package does not provide a suitable method to impose the experimental boundary conditions along the nonloaded edges in the presence of large displacements. Therefore in order to constrain these lateral edges to remain straight but free to move in-plane, fictitious beam elements with high in-plane bending stiffness but negligible torsional and axial stiffness were added along each edge.

The load-shortening curve obtained with this analysis is shown in Fig. 6. The model buckled into five half-waves (Fig. 7a) as observed in Stein's experiment, at the load of 13.6 kN, which is in excellent agreement with the experimental buckling load of 13.7 kN. The analysis could also predict the first mode switch into a six-half-wave configuration (Fig. 7b), but then failed to converge at the next critical point. The load-shortening curve is in good agreement with the experimental data within the elastic range, even if the numerical load level at which the mode jump occurs is 15% lower than the experimental one. A similar gap between experimental and numerical mode-switch load was observed in the analysis of the same problem carried out by Riks et al.[7] using a different technique. An investigation into the effect of the imperfection amplitude on mode switching showed that, considering the imperfection given in Eq. (21) with a range of values $0.001 < \alpha < 0.1$, the variation of the load of the captured mode switch was within $\pm 4\%$ of the load shown in Fig. 6

In the numerical results shown in Fig. 6, the two stable branches after buckling correspond to the deformation modes with five and six buckles respectively, the amplitude of which grows evenly with increasing load. These branches are connected by an unstable equilibrium path (the snap-back phase), along which a new buckle stems from a loaded edge.

Blade-Stiffened Composite Panel

Stiffened panels, widely used in airframe construction, are typically susceptible to mode jumping in their postbuckling regime. Here the case of a blade-stiffened composite panel tested to failure by Falzon et al.[6] is considered. The panel was manufactured from unidirectional prepreg T800/924C with material properties as shown in Table 1 and had dimensions of 538×728 mm with 2.75-mm skin thickness. Four blade stiffeners with tapered flanges were bonded to the skin using a film adhesive, such that the central bay was twice as wide as the outer bays. The two edges to be loaded were first potted in a resin and fiberglass mixture to prevent brooming, which resulted in a practically clamped-end loading condition for the panel. The panel was observed to buckle in a four half-wave mode shape (Fig. 8a) at 105 kN and subsequently underwent a dramatic mode

Table 1 Material properties for T800/924C unidirectional composite

Property	Value
Longitudinal tensile modulus	162 GPa
Longitudinal compressive modulus	145 GPa
Transverse tensile modulus	9.2 GPa
Transverse compressive modulus	9.5 GPa
In-plane shear modulus	5.0 GPa
Poisson's ratio	0.3 GPa
Longitudinal tensile strength	2.7 GPa
Longitudinal compressive strength	1.65 GPa
Transverse tensile strength	55 MPa
Transverse compressive strength	225 MPa
In-plane shear strength	100 MPa

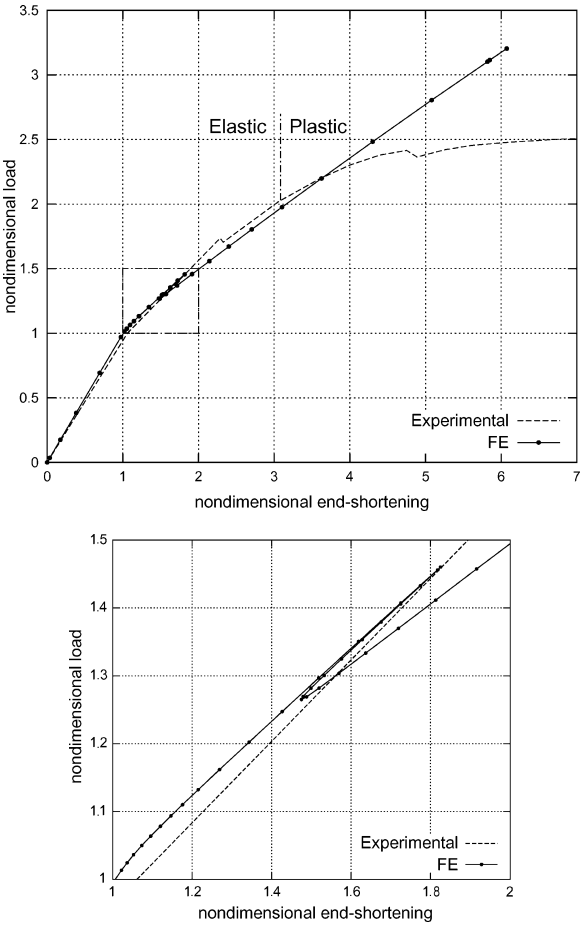

Fig. 6 Numerical analysis of Stein's aluminum panel, compared with experimental results: a) load vs end-displacement curve and b) detail of snap-back phase.

jump to five half-waves at 545 kN (Fig. 8b) before failing at 601 kN. A fractographic analysis showed that damage initiated at the free edge of the stiffener webs at midspan.

A finite element model of the panel was developed using LUSAS. As for the preceding example, an initial geometric imperfection equivalent to a combination of the first two eigenmodes was added to the perfect structure, and arc-length control was employed. In Fig. 9 the numerical load vs end-displacement curve is compared with the experimental one, from which it can be noted that the model was able to simulate the behavior of the real panel. The model's primary buckling mode had four half-waves (Fig. 10a), which then switched to five (Fig. 10b) before reaching a limit point at 601 kN. The failure mechanism of the model appears in the form of overall buckling of the panel, which causes excessive twisting of the stiffener webs at midspan (Fig. 10c). The numerical prediction is consistent with the observed delamination of the stiffener webs,[6] which precipitated catastrophic collapse. The clamped boundary

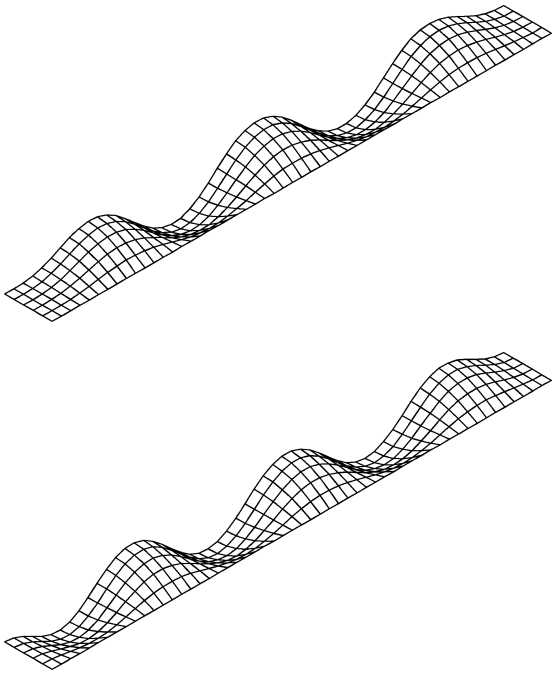

Fig. 7 Stein's plate a) before and b) after a mode jump (symmetric model).

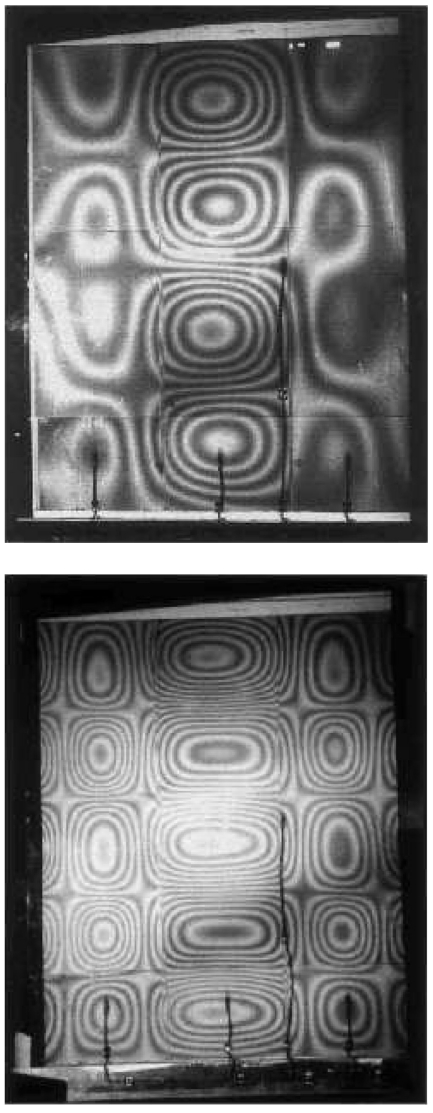

Fig. 8 Moiré fringe patterns of blade-stiffened panel.

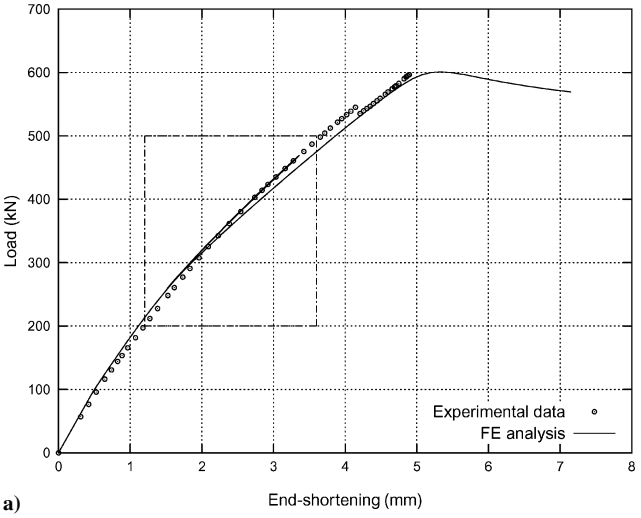

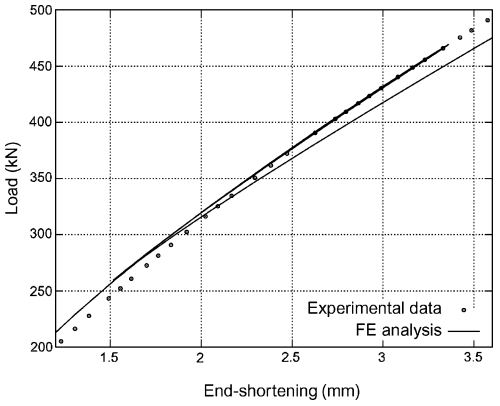

Fig. 9 Numerical analysis of the compression test of a blade-stiffened composite panel, compared with experimental results: a) load-shortening curve and b) detail of snap-back phase.

conditions did not require special techniques or the use of high-stiffness elements as in the preceding example, and the arc-length method was able to capture the mode switch without difficulty. The occurrence of mode jumping, however, was predicted at a 13.4% lower load than observed experimentally.

Improvement to "Standard" Arc-Length Methods

At the end of a predictor-corrector phase, the solution that is obtained is as close to the actual equilibrium path as the convergence tolerance allows, but in principle does not lie on the path exactly. There are situations in which not accounting for that residual can prevent convergence: this is more likely to occur in the vicinity of limit points with very sharp snap-backs, as is the case of some mode-jumping problems in postbuckling structures.

Mode jumping is a dynamic event that is triggered when the current configuration of a structure ceases to be stable under an increasing load. The structure undergoes a dynamic jump to a different stable configuration, allowing it to sustain higher loads. Although this phenomenon is dynamic in nature, quasi-static arc-length procedures can be successful at detecting a new stable equilibrium path beyond this secondary instability, provided an unstable equilibrium branch exists that connects the two states before and after a mode jump.

It is apparent that, from a quasi-static point of view, a mode switch corresponds to a secondary bifurcation of the current equilibrium path. A method to handle problems with bifurcations, without having to interrogate the critical points, is to eliminate bifurcations by adding an initial imperfection. Such imperfections should be small to reflect the likely imperfections of a real structure. In doing so, bifurcation points are transformed to limit points, but these can be very "sharp" because of the small imperfection size.

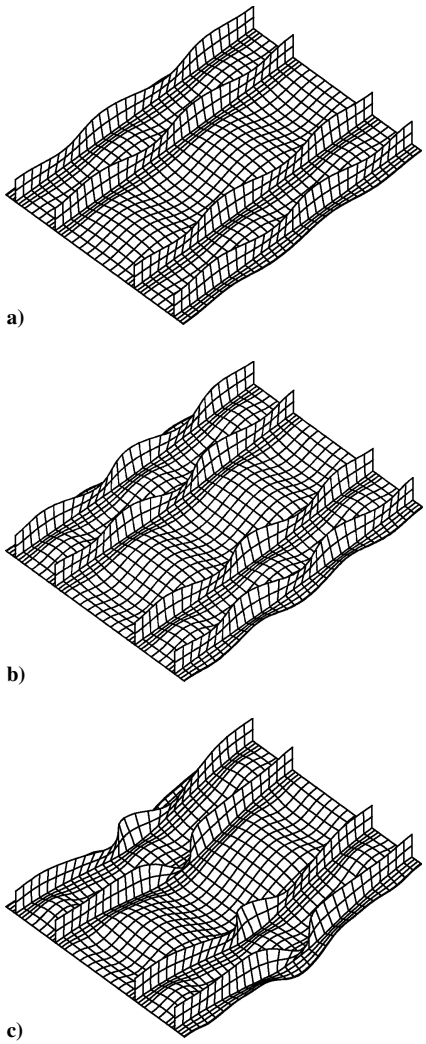

Fig. 10 Deformation modes of composite stiffened panel a) after primary buckling, b) after secondary buckling, and c) at final failure.

In the following, Crisfield's method will be considered, but similar concepts can be applied to other arc-length methods. A linearization of equilibrium equation (1) that accounts for the initial residual resembles Eq. (5) used in correctors, where predictor changes $\delta \boldsymbol{u}_1$, $\delta\lambda_1$ replace corrector changes:

$$\boldsymbol{g} + \boldsymbol{K}_t \delta \boldsymbol{u}_1 - \bar{\boldsymbol{r}} \delta\lambda_1 = \boldsymbol{0} \tag{22}$$

Expressing $\delta \boldsymbol{u}_1$ as a function of $\delta\lambda_1$:

$$\delta \boldsymbol{u}_1 = \delta\tilde{\boldsymbol{u}} + \delta\lambda_1 \hat{\boldsymbol{u}} \tag{23}$$

and substituting into the predictor constraint (9) yields the scalar equation

$$a_1 \delta\lambda_1^2 + a_2 \delta\lambda_1 + a_3 = 0 \tag{24}$$

where

$$a_1 = \hat{\boldsymbol{u}} \cdot \hat{\boldsymbol{u}} + \psi^2 \bar{\boldsymbol{r}} \cdot \bar{\boldsymbol{r}} \tag{25}$$

$$a_2 = 2\hat{\boldsymbol{u}} \cdot \delta\tilde{\boldsymbol{u}} \tag{26}$$

$$a_3 = \delta\tilde{\boldsymbol{u}} \cdot \delta\tilde{\boldsymbol{u}} - \Delta l^2 \tag{27}$$

If $\delta\tilde{\boldsymbol{u}} = -\boldsymbol{K}_t^{-1}\boldsymbol{g}$ is neglected, coefficient a_2 becomes zero, and with $\psi = 0$ the solutions $\delta\lambda_1$ are given by Eq. (16). It is not generally true, however, that both predictor solutions will have opposite signs, if the residual within the convergence limit is not discarded between increments. This is illustrated in Fig. 11 for a one-dimensional system under spherical constraint.

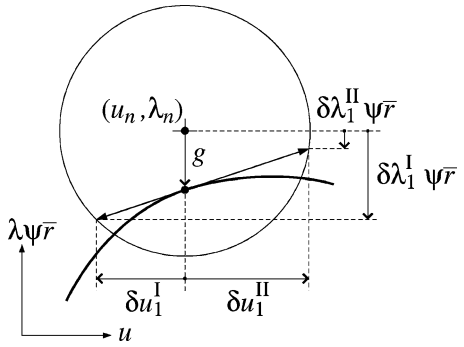

Fig. 11 Effect of residual force on predictor solutions near a limit point.

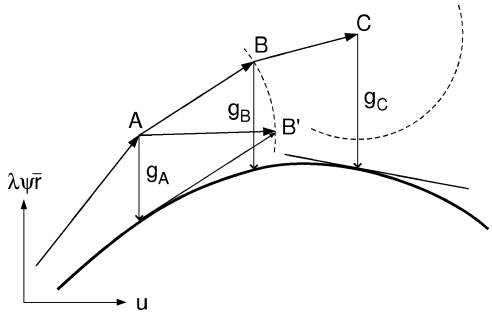

Fig. 12 Failure of spherical arc-length method at a limit point.

In Fig. 12 it is shown how an arc-length method can fail near a limit point. If A is a converged solution and the residual force is not accounted for in the predictor, the equilibrium path follows A-B rather than A-B', where the residual at B is still within the tolerance. When $\boldsymbol{g}$ becomes larger than the set tolerance (point C) and a second iteration is required, the arc-length constraint no longer intersects the equilibrium path, and any arc-length size reductions would be of no use. In the more general case of a multidimensional problem, it can be inferred from Eq. (23) that the direction of the displacement increment in the vicinity of a limit point, that is, when $\delta\lambda_1 \approx 0$, is almost entirely dependent on the residual $\boldsymbol{g}$. If this is neglected, the algorithm might not be able to find a direction along which convergence is achieved, despite several step reductions being carried out. A numerical example demonstrates this case in the next section.

A consequence of including $\boldsymbol{g}$ in the predictor is that predictor criteria based solely on the sign of $\delta\lambda_1$ are no longer suitable. The new criterion suggested here differs from the traditional ones in that it aims to find the solution that doubles back, rather than the one that goes forward, as it is considered easier to identify because it is almost equal and opposite to the preceding increment. Once identified, it is rejected, and the other solution is retained. Considering only the displacement space, the unit vector of the predictor corresponding to either solution $\delta\lambda_1$ is subtracted from the unit vector of the preceding converged increment. The Euclidean norm of the resultant should be approximately two for the solution that doubles back; therefore, the load factor increment that gives the smaller value of such norm is chosen:

$$\left\| \frac{\Delta \boldsymbol{u}_p}{\|\Delta \boldsymbol{u}_p\|} - \frac{\delta \boldsymbol{u}_1}{\|\delta \boldsymbol{u}_1\|} \right\| \ll 2 \tag{28}$$

In agreement with Crisfield's work,[12] the load terms controlled by ψ have not proved necessary. Nevertheless, when their contribution was accounted for, the following scaling parameter was successfully employed:

$$\psi = 1/\|\mathrm{diag}(\boldsymbol{K}_{\mathrm{el}})\| \tag{29}$$

Here ψ is given the dimension of the inverse of a stiffness, in order to make load and displacement terms comparable in magnitude. As a reference scalar stiffness value for the structure, the Euclidean norm of the main diagonal of its initial elastic stiffness matrix is used, being $\boldsymbol{K}_{\text{el}} \equiv \boldsymbol{K}_t(\boldsymbol{u} = \boldsymbol{0})$.

Simple Bar-Spring Model

To better understand some of the difficulties encountered in the application of arc-length methods to the study of mode jumping, the simple model of Fig. 13, originally proposed by Stein,[26] was chosen. Despite the small number of degrees of freedom, this system exhibits all of the main features of a postbuckling plate undergoing mode jumping, and an analytical solution proposed by Stein[26] is also available.

The structure consists of three rigid bars that are initially aligned, connected to each other by linear torsional springs with rotational stiffness C and laterally supported by nonlinear extensional springs. The restoring force on the extensional springs is proportional to the cube of their extension, and their stiffnesses are denoted by K and K_1, as shown in Fig. 13. By analyzing the total potential energy of this system Stein determined all possible equilibrium configurations and the relevant ranges of stability, and concluded that, during a loading process, the current equilibrium configuration is maintained until it becomes unstable, at which point the structure seeks for another stable equilibrium configuration. Stein also investigated the effect of an initial geometric imperfection and provided solutions in the case of a symmetric and an asymmetric imperfection.

The analytical study showed that the column buckles in a symmetric half-wave mode with $w_1 = w_2$ (Fig. 14a), which becomes unstable at an end-displacement $\Delta = 4C/l^3K_1$; at this point the structure snaps to a stable antisymmetric configuration with $w_1 = -w_2$ (Fig. 14b). The transition between these two modes occurs along an unstable equilibrium path, which in the displacement space has the elliptical form:

$$3K_1(w_1 + w_2)^2 + 16(w_1 - w_2)^2 = \text{const} \tag{30}$$

A finite element program was developed to obtain a numerical solution through arc-length control. The finite element program can model a structure of truss elements that are considered axially deformable; elements can be connected to each other by means of linear rotational springs and supported by nonlinear extensional springs applied either at an end node or at the midpoint of each truss. The restoring force of each extensional spring can be given an arbitrary cubic function of its extension. The program uses Green–Lagrange strains and total-Lagrangian formulation to allow for large displacements and rotations.

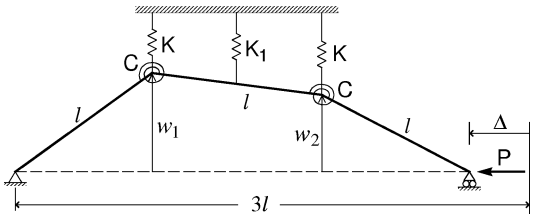

Fig. 13 Three-bar column connected by linear rotational springs and laterally restrained by nonlinear extensional springs.

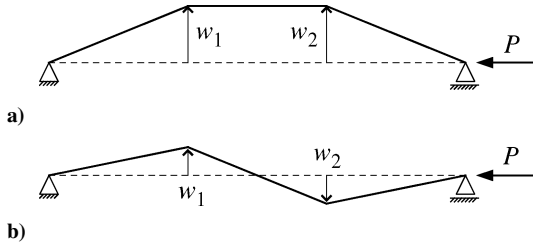

Fig. 14 Stable postbuckling deformation modes of three-bar column.

The three-element column with stiffness ratio $K_1/K = 1$ was modeled using this finite element program. To eliminate bifurcations, a slightly asymmetric initial imperfection was added, with amplitude $w_{1,0} = 0.1001\sqrt{(C/Kl^2)}$, $w_{2,0} = 0.1\sqrt{(C/Kl^2)}$. The truss-elements axial stiffness was set very high (10^6 K) for simulating rigid bars. As a consequence, the configuration of the finite element model can be considered almost fully determined by the transversal displacements w_1 and w_2, analogous to the analytical model. Both the standard predictor in Eq. (16) and the improved predictor in Eq. (24) were applied.

Using the improved predictor and corresponding criterion [Eq. (28)], the full equilibrium path was obtained, as shown in Fig. 15 in a displacement-load space. As for the analytical perfect model, the equilibrium path is characterized by three postbuckling phases. In the first phase, after buckling the structure bends in a symmetric mode (in the plane $w_1 = w_2$), up to a limit load. The second phase is a transition from the symmetric to the antisymmetric mode ($w_1 = -w_2$) and is an unstable branch because the load factor decreases; during this stage, the displacement coordinates describe a curve in the (w_1, w_2) space that is almost elliptic. In the third phase the structure progressively tends to assume the antisymmetric configuration, moving along a stable branch. The equilibrium path is qualitatively the same as that shown by Everall and Hunt[27] for struts and plates, where w_1 and w_2 are replaced by the amplitudes of the two modes before and after a mode change. The load vs end-displacement curve shown in Fig. 16 highlights the snap-back behavior of Stein's system.

The use of the standard predictor causes the incremental procedure to fail in the vicinity of the limit point, as shown in Fig. 17. Here predictor and corrector steps performed by either procedure near this critical state are shown. Whereas the improved predictor is able to overcome the limit point simply by reducing the step arc

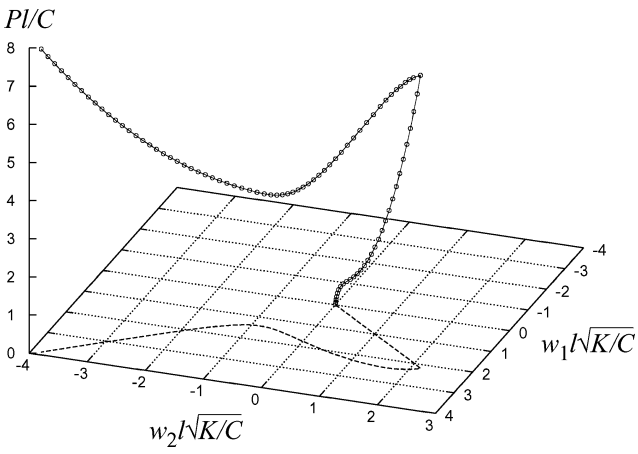

Fig. 15 Equilibrium path of Stein's three-element column.

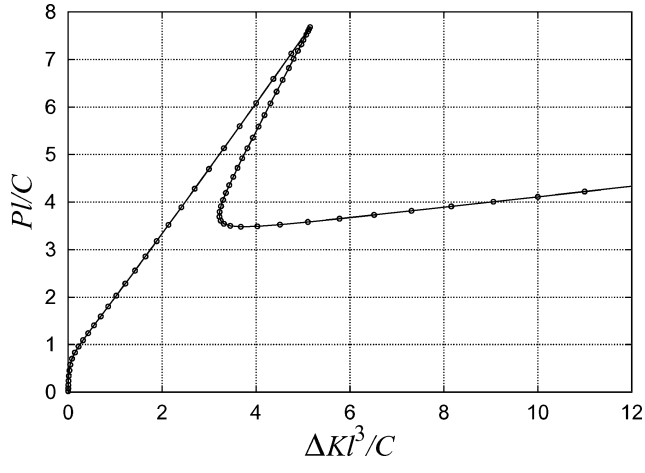

Fig. 16 Load-shortening curve of Stein's column.

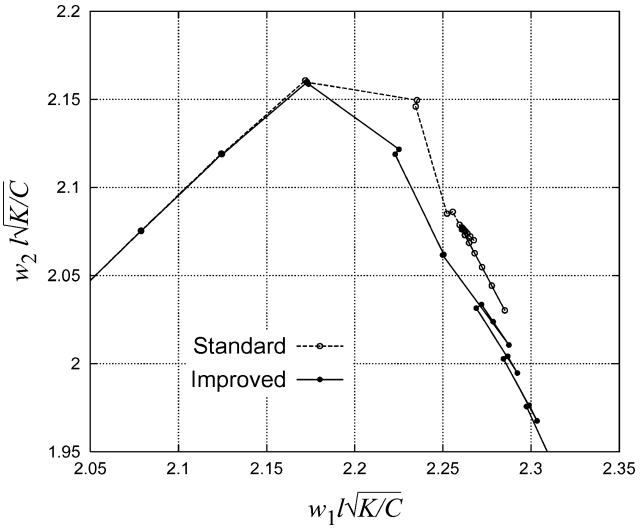

Fig. 17 Equilibrium path traced by standard and improved algorithms around a limit point.

length when necessary, the traditional predictor is unable to find the correct direction, even if several step reductions are performed. In particular it is noted that, despite the almost identical configuration that either technique achieves at the turning point, the predicted direction of increment is totally different.

Conclusions

The arc-length method can be a useful tool for gaining insight into the postbuckling regime of a structure, in particular when mode changes are likely to occur. Although mode jumps often manifest themselves as abrupt dynamic phenomena, in some cases the use of the arc-length method for solving the relevant quasi-static numerical problem has proved able to predict the postjump deformation mode, by following an unstable equilibrium path after the stability threshold of the current mode is reached, which eventually leads to the new configuration. The analysis of a postbuckling stiffened composite panel showed the same behavior as the relevant experimental test, albeit the mode jump was predicted at a 14% lower load level.

The use of a quasi-static procedure is considerably more efficient in terms of computational costs when compared with a dynamic approach. However it is not thoroughly robust, and much depends on the nature and severity of the critical points encountered along the equilibrium path. As the analysis of an isotropic rectangular plate demonstrated, the arc-length method was not able to overcome the limit point on the six-half-wave branch and therefore to predict the subsequent switches into seven and eight half-wave modes observed in the experiment. This failure is thought to be related with the way the boundary condition of uniform in-plane displacement along the nonloaded side of the plate was enforced.

The possible presence of bifurcations along an equilibrium path has to be regarded with special attention. The arc-length method itself is not able to deal properly with these critical points. The proper way to treat bifurcations requires knowledge of the critical eigenvector (or eigenvectors, in case of multiple null eigenvalues) in order to determine the secondary branch onto which the system has to divert. From a quasi-static point of view, a mode jump appears as a bifurcation because it occurs when an equilibrium path corresponding to a deformation mode becomes unstable after encountering a secondary branch. By introducing geometric imperfections into the structure, bifurcation points are reduced to limit points. For this approach to be effective, a suitable imperfection has to be chosen, which eliminates all bifurcations. A drawback of this technique, however, is that the result might depend on the imperfection employed, either in terms of load level of jumps, or also of postjump configuration modes, especially when there are multiple postcritical equilibrium configurations.

Although adding a geometric imperfection can eliminate bifurcations, limit points that are generated in their place can feature a very sharp snap-back, which can yield numerical difficulties and therefore prevent convergence, as demonstrated by the analysis of a rectangular plate and also by the simple bar-spring model undergoing mode jumping. Standard formulations of the arc-length method need to be improved to be more effective at overcoming sharp limit points. Indeed it has been shown that an improved formulation that accounts for the residual at the beginning of each increment enables the capturing of mode switching in the bar-spring model, whereas standard methods that neglect the residual fail. This improved formulation invalidates the standard criteria for selecting the correct load parameter at the predictor stage, which is essential for this procedure's success; therefore, a new technique was used.

References

[1]Stein, M., "Loads and Deformations of Buckled Rectangular Plates," NASA TR R-40, 1959.

[2]Minguet, P. J., Dugundji, J., and Lagace, P., "Postbuckling Behavior of Laminated Plates Using a Direct Energy-Minimization Technique," *AIAA Journal*, Vol. 27, No. 12, 1989, pp. 1785–1792.

[3]Starnes, J. H., Jr., Knight, N. F., Jr., and Rouse, M., "Postbuckling Behavior of Selected Flat Stiffened Graphite-Epoxy Panels Loaded in Compression," *AIAA Journal*, Vol. 23, No. 8, 1985, pp. 1236–1246; also AIAA Paper 82-0777, 1982.

[4]Stevens, K. A., Ricci, R., and Davies, G. A. O., "Buckling and Postbuckling of Composite Structures," *Composites*, Vol. 26, No. 3, 1995, pp. 189–199.

[5]Falzon, B. G., and Steven, G. P., "Buckling Mode Transition in Hat-Stiffened Composite Panels Loaded in Uniaxial Compression," *Composite Structures*, Vol. 37, No. 2, 1997, pp. 253–267.

[6]Falzon, B. G., Stevens, K. A., and Davies, G. O., "Postbuckling Behaviour of a Blade-Stiffened Composite Panel Loaded in Uniaxial Compression," *Composites Part A: Applied Science and Manufacturing*, Vol. 31, No. 5, 2000, pp. 459–468.

[7]Riks, E., Rankin, C. C., and Brogan, F. A., "On the Solution of Mode Jumping Phenomena in Thin-Walled Shell Structures," *Computer Methods in Applied Mechanics and Engineering*, Vol. 136, Nos. 1–2, 1996, pp. 59–92.

[8]Bushnell, D., Rankin, C. C., and Riks, E., "Optimization of Stiffened Panels in Which Mode Jumping is Accounted for," *Stability Analysis of Plates and Shells—A Collection of Papers in Honor of Dr. Manuel Stein*, NASA CP-1998-206280, 1998, pp. 105–145.

[9]Falzon, B. G., and Hitchings, D., "Mode-Switching in Postbuckling Composite Aerostructures," *Proceedings of the 2nd International Conference on Structural Stability and Dynamics*, World Scientific, Singapore, 2003, pp. 459–464.

[10]Wempner, G. A., "Discrete Approximations Related to Nonlinear Theories of Solids," *International Journal of Solids and Structures*, Vol. 7, No. 11, 1971, pp. 1581–1599.

[11]Riks, E., "An Incremental Approach to the Solution of Snapping and Buckling Problems," *International Journal of Solids and Structures*, Vol. 15, No. 7, 1979, pp. 529–551.

[12]Crisfield, M. A., "A Fast Incremental/Iterative Solution Procedure that Handles 'Snap-Through,'" *Computers and Structures*, Vol. 13, Nos. 1–3, 1981, pp. 55–62.

[13]Fried, I., "Orthogonal Trajectory Accession to the Nonlinear Equilibrium Curve," *Computer Methods in Applied Mechanics and Engineering*, Vol. 47, No. 3, 1984, pp. 283–297.

[14]Riks, E., "The Application of Newton's Method to the Problem of Elastic Stability," *Journal of Applied Mechanics*, Vol. 39, No. 4, 1972, pp. 1060–1065.

[15]Batoz, J. L., and Dhatt, G., "Incremental Displacement Algorithms for Non-Linear Problems," *International Journal for Numerical Methods in Engineering*, Vol. 14, No. 8, 1979, pp. 1262–1266.

[16]Hellweg, H.-B., and Crisfield, M. A., "A New Arc-Length Method for Handling Sharp Snap Backs," *Computers and Structures*, Vol. 66, No. 5, 1998, pp. 704–709.

[17]De Souza Neto, E. A., and Feng, Y. T., "On the Determination of the Path Direction for Arc-Length Methods in the Presence of Bifurcations and 'Snap-Backs,'" *Computer Methods in Applied Mechanics and Engineering*, Vol. 179, Nos. 1–2, 1999, pp. 81–89.

[18]Cerini, M., and Falzon, B. G., "The Reliability of the Arc-Length Method in the Analysis of Mode-Jumping Problems," AIAA Paper 2003-1621, April 2003.

[19]Ragon, S. A., Gürdal, Z., and Watson, L. T., "A Comparison of Three Algorithms for Tracing Nonlinear Equilibrium Paths of Structural Systems," *International Journal of Solids and Structures*, Vol. 39, No. 3, 2002, pp. 689–698.

[20]Shin, D. K., Griffin, O. H., Jr., and Gürdal, Z., "Postbuckling Response of Laminated Plates Under Uniaxial Compression," *International Journal of Non-Linear Mechanics*, Vol. 28, No. 1, 1993, pp. 95–115.

[21]Stoll, F., "Analysis of the Snap Phenomenon in Buckled Plates," *International Journal of Non-Linear Mechanics*, Vol. 29, No. 2, 1994, pp. 123–138.

[22]Stoll, F., and Olson, S. E., "Finite Element Investigation of the Snap Phenomenon in Buckled Plates," *Stability Analysis of Plates and Shells—A Collection of Papers in Honor of Dr. Manuel Stein*, NASA CP-1998-206280, 1998, pp. 435–444.

[23]Everall, P. R., and Hunt, G. W., "Arnold Tongue Predictions of Secondary Buckling in Thin Elastic Plates," *Journal of Mechanics and Physics of Solids*, Vol. 47, No. 10, 1999, pp. 2187–2206.

[24]*LUSAS, Theory Manual*, Ver. 13.4, FEA, Ltd., Kingston-upon-Thames, England, U.K., 2002.

[25]Irons, B. M., "The SemiLoof Shell Element," *Finite Elements for Thin Shells and Curved Members*, edited by D. G. Ashwell and R. H. Gallager, Wiley, London, 1976, Chap. 11.

[26]Stein, M., "The Phenomenon of Change in Buckle Pattern in Elastic Structures," NASA TR R-39, 1959.

[27]Everall, P. R., and Hunt, G. W., "Mode Jumping in the Buckling of Struts and Plates: A Comparative Study," *International Journal of Non-Linear Mechanics*, Vol. 35, No. 6, 2000, pp. 1067–1079.

B. Sankar
Associate Editor